Hadron-quark phase transition in asymmetric matter with boson condensation

Rafael Cavagnoli
Departamento de Física, CFM, Universidade Federal de Santa Catarina, Florianópolis, SC, C.P. 476, CEP 88.040-900, Brazil and Centro de Física Computacional, Departamento de Física, Universidade de Coimbra, P-3004-516 Coimbra, Portugal

Constança Providência
Centro de Física Computacional, Departamento de Física, Universidade de Coimbra, P-3004-516 Coimbra, Portugal

Debora P. Menezes
Departamento de Física, CFM, Universidade Federal de Santa Catarina, Florianópolis, SC, C.P. 476, CEP 88.040-900, Brazil
(Received 17 September 2010; published 11 April 2011)

In the present work we study the hadron-quark phase transition with boson condensation in asymmetric matter by investigating the binodal surface and extending it to finite temperature to mimic the QCD phase diagram. We consider a system with two conserved charges (isospin and baryon densities) using the Gibbs' criteria for phase equilibrium. To obtain these conditions we use two different models for the two possible phases, namely, the nonlinear Walecka model (NLWM) for the hadron matter (also including hyperons) and the MIT bag model for the quark phase. It is shown that the phase transition is very sensitive to the density dependence of the equation of state and the symmetry energy. For an isospin asymmetry of 0.2 and a mixed phase with a fraction of 20% of quarks, a transition density in the interval $2\rho_0 < \rho_t < 4\rho_0$ was obtained for temperatures $30 < T < 65$ MeV.

DOI: 10.1103/PhysRevC.83.045201 PACS number(s): 21.65.−f, 25.75.Nq, 05.70.Fh, 12.38.Mh

I. INTRODUCTION

Since some decades ago just after the discovery of the asymptotic freedom of QCD [1] the possibility of the existence of a new state of matter in high-energy physics is under consideration, namely, a color deconfined phase of quarks and gluons, the so-called quark-gluon plasma (QGP) [2]. The main goal of the heavy-ion collision experiments at ultrarelativistic energies is to create, under controlled conditions, and understand the properties of this new state of matter. This opens a new field of study in strong interaction physics.

Many experiments have been proposed and accelerators have been built in the search for QGP at different energies at SIS/GSI, AGS/BNL, SPS/CERN, RHIC/BNL, and LHC/CERN to look for some signs and signatures of the production of QGP that subsequently hadronizes [3]. The study of particle production in ion collisions contributes to the understanding of the conditions under which QGP may be produced and also to determine the equations of state (EOS) of strongly interacting matter.

In hydrodynamical models the system that arises from a high-energy collision (fireball) reaches an approximately local thermal equilibrium (thermalization) and expands, evolving collectively up to the point when the mean free path of the created and interacting particles becomes large enough for the particles to escape from the fluid; i.e., the interactions among the particles of the system cease because the system has reached the freeze-out point. The approximately local thermalization is considered to be due to detailed computations of the expansion stage that takes much longer than the typical scattering times [4]. Although, nonequilibrium processes are also important for the dynamics, equilibrium processes are a quite good approximation to be used in theoretical models and are a reasonable first approximation at freeze-out. Some authors consider both the temperature at which the inelastic collisions cease (chemical freeze-out) and the temperature at which the elastic collisions cease (kinetic freeze-out) [5].

At the end of the eighties of the last century the existence of the (chiral) critical end point (CEP) in the QCD phase diagram was suggested [6,7] and since then its properties have been extensively studied [8]. Although, most lattice QCD calculations indicate the existence of the CEP for $\mu_B > 160$ MeV [9–11], its exact location is not well known since it depends, for example, on the mass of the strange quark. The CEP separates the second-order transitions at high temperatures (or even a smooth crossover) from the first-order transitions at high chemical potentials in the QCD phase diagram. However, according to the findings of Ref. [12] there might not even exist a chiral critical point. Studying this intermediate region is a hard task since perturbation theory cannot be applied to QCD at this regime and additionally at finite chemical potential the usual lattice approach fails. Moreover, new techniques have been proposed to study lattice QCD at finite T and μ [13]. On the other hand the lattice QCD simulations of different groups disagree with each other on the location of the CEP.

Subsequently in the late nineties a hypothesis arose [14] that the onset of the deconfinement phase transition was located between the top AGS and SPS energies. The CERN energy scan program of the NA49 experiment at SPS has given signs of a phase change at $E_{\rm lab} \sim 30$ A GeV particularly from the hornlike peak in the K^+/π^+ ratio [15].

Furthermore, the hadronic freeze-out estimated for different colliding energies [16] shows a maximum at $\sqrt{s_{NN}} = 4 + 4$ GeV, which can be reached for a fixed-target bombarding energy of 20–30 A GeV at the baryonic chemical potential region $\mu_B = 400$–500 MeV. In addition, hydrodynamical

TABLE I. Ion beam top energies in some collision experiments.

	SIS/GSI	Synchr./JINR	AGS/BNL	↓	SPS/CERN	RHIC/BNL	LHC/CERN
$E_{\rm lab}$ (A GeV)	2.0	4.2	14.6		158	2.1×10^4	1.6×10^7
$\sqrt{s_{NN}}$ (GeV)	2.7	3.4	5.6		17.3	200	5400
			FAIR/GSI		NICA/JINR		
$E_{\rm lab}$ (A GeV)			34		40	(← planned facilities)	
$\sqrt{s_{NN}}$ (GeV)			8.2		9		

calculations [17,18] of phase trajectories during collisions, in the QCD phase diagram, indicate that for $E_{\rm lab} \sim 30$ A GeV ($\sqrt{s_{NN}} \sim 8$ GeV) the trajectory goes near the CEP.

Since then, the interest in the intermediate energies (not ultrarelativistic) in collision experiments has increasd as well as the theoretical study of the phase transition in that regime.

For this purpose the new facilities, namely, the Nuclotron-based ion collider facility (NICA) at JINR/Dubna [19] and the Facility for Antiproton and Ion Research (FAIR) at GSI/Darmstadt [20], give the opportunity to explore an interesting region of the phase diagram, in search of QGP and where the CEP is expected to exist, complementing other heavy-ion collision experiments (NA61-SHINE, low-energy RHIC) compatible with the energy range $E_{\rm lab} = 2$–40 A GeV. It is also important to consider the possibility that new features arise at still lower temperatures and higher densities as the color superconducting quark matter phases like the CFL (color-flavor locked) phase [21] and the recently conjectured quarkyonic phase [22]. Different possible patterns for color superconductivity have been conjectured (see e.g., Ref. [23] and references therein). However, in the present work we do not consider these phases. A summary of ion beam top energies used in some collision experiments is shown in Table I.

It is also possible to study the phase transition from hadronic matter to a quark phase within the effective models that describe two separated phases, and also the structure of the mixed phase can be obtained through the Gibbs' conditions [24]. Some features of this phase transition can be obtained by means of the binodal surface, which is a phase coexistence curve in the parameter space.

The different ion beams used in collision experiments present different numbers of neutrons (N) and protons (Z). It is also interesting to study the isospin effects on the transition to a mixed phase of hadrons and quarks. We can define the asymmetry parameter (isospin ratio) of a nucleus (or the hadron phase) as $\alpha \equiv (N - Z)/(N + Z)$, such that α runs from 0 (symmetric matter) to 1 (pure neutron matter). From Table II one sees some ions used in nucleus-nucleus collisions and the respective asymmetry parameter of each system. Systems with isospin ratios $0 \leqslant \alpha \leqslant 0.23$ are up to now experimentally accessible in ion collisions and the case $\alpha = 1.0$ corresponds to neutron matter which is relevant in some astrophysical applications.

We study the phase transition from hadrons to a QGP in asymmetric matter using a two-phase model, analyzing the features that depend on the isospin and may be relevant in a phenomenological description of heavy-ion collisions [25–28].

It is interesting to investigate asymmetric systems since in the liquid-gas phase transition of nuclear matter the asymmetric case shows different properties from the symmetric one [25,29,30]. It is shown that the transition of an asymmetric system is of the second order (continuous) rather than the first-order (discontinuous) as in symmetric systems [25–28].

Hence, an interesting task is to investigate the isospin effect on the hadron-quark phase transition at lower temperatures and densities higher than the saturation density of the normal nuclear matter, which can be probed in heavy-ion collisions at intermediate energies. In addition, the presence of bosons can modify the isospin of the hadron phase. Also, at low temperatures these features depend strongly on the nuclear symmetry energy. On the other hand, at higher temperatures the inclusion of bosons shows an interesting feature due to the onset of a boson condensate in asymmetric systems if we consider an approximately local thermal equilibrium.

This approach is useful for providing a qualitative orientation on the features that arise when a phase transition from hadrons to quarks takes place and two conserved charges are considered, i.e., at finite baryon density and isospin.

As already mentioned, the problem we investigate in the present paper has already been studied in previous works [26–28] within different perspectives, based on different parametrizations and containing different ingredients. In Ref. [26] the hadronic phase is given by one parametrization of the nonlinear Walecka model, the quark phase is calculated with the MIT bag model for one specific value of the bag constant, and pions are included. In Refs. [27,28] a mixed phase of hadrons and quarks is particularly emphasized and the influence of the symmetry energy on the phase transition is investigated. In Ref. [28] neither bosons nor gluons are considered and the quark phase is described within the MIT

TABLE II. Some ions used in collision experiments and the respective asymmetry parameter (α) of the system.

	$^{12}C + {}^{12}C$	$^{20}Ne + {}^{20}Ne$	$^{58}Ni + {}^{58}Ni$
α	0	0	0.034
	$^{20}Ne + {}^{63}Cu$	$^{20}Ne + {}^{118}Sn$	$^{118}Sn + {}^{118}Sn$
α	0.060	0.130	0.150
	$^{20}Ne + {}^{209}Bi$	$^{197}Au + {}^{197}Au$	$^{20}Ne + {}^{238}U$
α	0.188	0.198	0.201
	$^{197}Au + {}^{208}Pb$	$^{208}Pb + {}^{208}Pb$	$^{238}U + {}^{238}U$
α	0.205	0.211	0.227

bag model, and in Ref. [27] two different quark models are used: the MIT bag model (with and without gluons) and the color dielectric quark model. In these works five different parametrizations of the nonlinear Walecka model are considered and one of them includes the δ mesons. All these models have a quite high value of the symmetry energy slope, namely, $85 < L < 103$ MeV, and therefore they have a quite hard symmetry energy at intermediate densities, the densities of interest for the present work.

In the present work we consider seven different parametrizations of the nonlinear Walecka model, which span a large variety of EOS: they include hard and soft EOS with hard and soft symmetry energies at intermediate densities. This allows us to see the effect of both the isoscalar and the isovector interaction on the phase transition. For the quark model we have considered the MIT bag model with various values of the bag constant and with gluons. The bag constant was chosen in accordance with heavy-ion collision data. In the hadronic phase we have studied the effect of including two kinds of bosons, pions and kaons. This more complete picture allows us to discuss various aspects of the phase transition at finite temperature which have not been discussed before.

The remainder of this article is organized as follows: In Sec. II we present the formalism used in this work. In Sec. III the mixed phase features are presented and in Sec. IV we show the numerical results and discussion. Finally, in Sec. V we summarize the results and give a brief concluding discussion.

II. THE FORMALISM

In the present section we present the EOS for the hadron phase and for the quark phase used in this work and their respective definitions. Bosons are included using a meson-exchange-type Lagrangian that couples the bosons to meson fields and the possibility of a boson condensate is also presented.

A. Quark phase: Quarks *u* and *d* (+ gluons)

Quark matter has been extensively described by the MIT bag model [31]. In its simplest form, the quarks are considered to be free inside a bag and the thermodynamic properties are derived from the Fermi gas model in two limits: $T = 0, m_q \neq 0$ and $T \neq 0, m_q = 0$. The energy density, the pressure, and the quark q density are, respectively, given by

$$\mathcal{E}_q = 3 \times 2 \sum_{q=u,d} \int \frac{d^3p}{(2\pi)^3} \sqrt{\mathbf{p}^2 + m_q^2} (f_{q+} + f_{q-}) + B, \quad (1)$$

$$P_q = \frac{1}{\pi^2} \sum_q \int dp \frac{\mathbf{p}^4}{\sqrt{\mathbf{p}^2 + m_q^2}} (f_{q+} + f_{q-}) - B, \quad (2)$$

$$n_q = 3 \times 2 \int \frac{d^3p}{(2\pi)^3} (f_{q+} - f_{q-}), \quad (3)$$

$$f_{q\pm} = \frac{1}{1 + e^{[(\epsilon_q \mp \mu_q)/T]}}, \quad (4)$$

where 3 stands for the number of colors, 2 stands for the spin degeneracy, m_q stands for the quark masses, B represents the bag pressure, $f_{q\pm}$ represents the distribution functions for the quarks and antiquarks, $\epsilon_q = \sqrt{\mathbf{p}_q^2 + m_q^2}$, $\pm\, \mu_q$ is the chemical potential for quarks and antiquarks of type q,

$$\mu_u = \frac{2\mu_p - \mu_n}{3}, \quad \mu_d = \frac{2\mu_n - \mu_p}{3}. \quad (5)$$

The quark density is

$$n_q = n_u + n_d, \quad (6)$$

and the "quark baryon density" is given by

$$n_B^Q = \frac{n_u + n_d}{3}. \quad (7)$$

The thermodynamic potential per unit volume of the MIT bag model (two-flavor case) and the corresponding EOS [26,32] for massless quarks and a Bose gas of gluons of degeneracy $\gamma_g = 2 \times 8$ with the lowest-order gluon interaction (α_s) is

$$\frac{\Omega_{\rm QGP}}{V} = -\frac{\pi^4}{45} T^4 \left(8 + \frac{21}{4} N_f\right) - \frac{1}{2} \sum_{q=u,d} \left(T^2 \mu_q^2 + \frac{\mu_q^4}{2\pi^2}\right) + \frac{2\pi}{9} \alpha_s \left[T^4 \left(3 + \frac{5}{4} N_f\right) + \frac{9}{2} \sum_{q=u,d} \left(\frac{T^2 \mu_q^2}{\pi^2} + \frac{\mu_q^4}{2\pi^4}\right)\right] + B, \quad (8)$$

from which we can obtain the pressure $P_{\rm QGP} = -\Omega_{\rm QGP}/V$, the energy density, and the quark number density:

$$P_{\rm QGP} = \frac{8\pi^2}{45} T^4 \left(1 - \frac{15\alpha_s}{4\pi}\right) + \sum_q \left[\frac{7}{60} \pi^2 T^4 \left(1 - \frac{50\alpha_s}{21\pi}\right) + \left(\frac{1}{2} T^2 \mu_q^2 + \frac{1}{4\pi^2} \mu_q^4\right) \left(1 - \frac{2\alpha_s}{\pi}\right)\right] - B, \quad (9)$$

$$\mathcal{E}_{\rm QGP} = 3P_{\rm QGP} + 4B;$$

$$n_q = \sum_q \left(T^2 \mu_q + \frac{\mu_q^3}{\pi^2}\right) \left(1 - \frac{2\alpha_s}{\pi}\right). \quad (10)$$

The strong coupling α_s is taken as a constant in the present work ($\alpha_s = 0.349$) and N_f stands for the number of flavors ($N_f = 2$, quarks u and d).

In fact the strange quark should have been included in the quark phase since, although we have in mind a zero net strangeness, at finite temperature strange quark-antiquark pairs will be formed. However, since we are mainly interested in high-density hadronic matter at a temperature below 70 MeV, the effect of including the strange quarks is negligible. We have verified that for $T = 60$ MeV and a baryonic density larger than 2 times the saturation density the contribution of the s quarks to the pressure is below 1%.

B. Hadron phase: Nucleons (+ hyperons)

The equations of state of asymmetric matter within the framework of the relativistic nonlinear Walecka model (NLWM) [33] are presented next. In this model the nucleons are coupled to neutral scalar σ, isoscalar-vector ω^μ, and

isovector-vector $\vec{\rho}^{\mu}$ meson fields. The Lagrangian density reads

$$\begin{aligned}\mathcal{L}_B &= \bar{\psi}[\gamma_\mu(i\partial^\mu - g_{\omega j}\omega^\mu - g_{\rho j}\vec{\tau}_j\cdot\vec{\rho}^\mu) - m_j^*]\psi \\ &+ \frac{1}{2}\partial_\mu\sigma\,\partial^\mu\sigma - \frac{1}{2}m_\sigma^2\sigma^2 - \frac{1}{3!}k\sigma^3 - \frac{1}{4!}\lambda\sigma^4 \\ &- \frac{1}{4}\Omega_{\mu\nu}\Omega^{\mu\nu} + \frac{1}{2}m_\omega^2\omega_\mu\omega^\mu + \frac{1}{4!}\xi g_\omega^4(\omega_\mu\omega^\mu)^2 \\ &- \frac{1}{4}\vec{R}_{\mu\nu}\cdot\vec{R}^{\mu\nu} + \frac{1}{2}m_\rho^2\vec{\rho}_\mu\cdot\vec{\rho}^\mu \\ &+ \Lambda_{\rm v}(g_\rho^2\vec{\rho}_\mu\cdot\vec{\rho}^\mu)(g_\omega^2\omega_\mu\omega^\mu), \end{aligned} \tag{11}$$

where $m_j^* = m_j - g_{\sigma j}\sigma$ is the baryon effective mass, $\Omega_{\mu\nu} = \partial_\mu\omega_\nu - \partial_\nu\omega_\mu$, $\vec{R}_{\mu\nu} = \partial_\mu\vec{\rho}_\nu - \partial_\nu\vec{\rho}_\mu - g_\rho\left(\vec{\rho}_\mu\times\vec{\rho}_\nu\right)$, g_{ij} are the coupling constants of mesons $i = \sigma, \omega, \rho$ with baryon j, and m_i is the mass of meson i. The couplings k ($k = 2M_N g_\sigma^3 b$) and λ ($\lambda = 6g_\sigma^4 c$) are the weights of the nonlinear scalar terms and $\vec{\tau}$ is the isospin operator. This Lagrangian includes an isoscalar-isovector mixing term $\Lambda_{\rm v}(g_\rho^2\vec{\rho}_\mu\cdot\vec{\rho}^\mu)(g_\omega^2\omega_\mu\omega^\mu)$ as presented in Ref. [34] that plays an important role in high densities. It can also be extended to include all the hyperons from the baryon octet.

Within the relativistic mean field (RMF) framework the thermodynamic potential per unit volume corresponding to the Lagrangian density (11) is

$$\begin{aligned}\frac{\Omega_B}{V} &= \frac{1}{2}m_\sigma^2\sigma_0^2 + \frac{1}{3!}k\sigma_0^3 + \frac{1}{4!}\lambda\sigma_0^4 - \frac{1}{2}m_\omega^2\omega_0^2 - \frac{1}{4!}\xi\omega_0^4 \\ &- \frac{1}{2}m_\rho^2\rho_{03}^2 - 2T\sum_j\int\frac{d^3p}{(2\pi)^3}\{\ln[1+e^{-\beta(E_j^*-\nu_j)}] \\ &+ \ln[1+e^{-\beta(E_j^*+\nu_j)}]\} - \Lambda_{\rm v}g_\rho^2g_\omega^2\omega_0^2\rho_{03}^2, \end{aligned} \tag{12}$$

where $\beta = 1/T$, $E_j^* = (\mathbf{p}_j^2 + M_j^{*2})^{1/2}$, and the effective chemical potential of baryon j is given by

$$\nu_j = \mu_j - g_\omega\omega_0 - \tau_{3j}g_\rho\rho_{03}. \tag{13}$$

The EOS for the baryons can then be calculated as

$$\begin{aligned}P_B &= \frac{1}{3\pi^2}\sum_j\int\frac{p^4dp}{\sqrt{p^2+m_j^{*2}}}(f_{Fj+}+f_{Fj-}) + \frac{m_\omega^2}{2}\omega_0^2 \\ &+ \frac{\xi}{24}\omega_0^4 + \frac{m_\rho^2}{2}\rho_{03}^2 - \frac{m_\sigma^2}{2}\sigma_0^2 - \frac{k}{6}\sigma_0^3 - \frac{\lambda}{24}\sigma_0^4 \\ &+ \Lambda_{\rm v}g_\rho^2g_\omega^2\omega_0^2\rho_{03}^2, \end{aligned} \tag{14}$$

$$\begin{aligned}\mathcal{E}_B &= \frac{1}{\pi^2}\sum_j\int p^2dp\sqrt{p^2+m_j^{*2}}(f_{Fj+}+f_{Fj-}) + \frac{m_\omega^2}{2}\omega_0^2 \\ &+ \frac{\xi}{8}\omega_0^4 + \frac{m_\rho^2}{2}\rho_{03}^2 + \frac{m_\sigma^2}{2}\sigma_0^2 + \frac{k}{6}\sigma_0^3 + \frac{\lambda}{24}\sigma_0^4 \\ &+ 3\Lambda_{\rm v}g_\rho^2g_\omega^2\omega_0^2\rho_{03}^2, \end{aligned} \tag{15}$$

$$n_B^j = \frac{2}{(2\pi)^3}\int(f_{Fj+} - f_{Fj-})\,d^3p. \tag{16}$$

Here, $f_{Fj\pm}$ is the Fermi distribution for the baryon (+) and the antibaryon (−) j:

$$f_{Fj\pm} = \frac{1}{e^{\beta(E_j^*\mp\nu_j)}+1}. \tag{17}$$

C. Hadron phase: Bosons (pions + kaons)

It is possible to include the boson fields using terms from the chiral perturbation theory [35]. In the present work we prefer to use a meson-exchange-type Lagrangian that couples the bosons to meson fields and for simplicity we apply the same approach to the kaons and pions.

An effective chiral Lagrangian like the one introduced by Kaplan and Nelson [35] could have been used to describe hadronic matter with pion and kaon condensation. However, the baryon sector is more easily described within a relativistic field theory of the Walecka type, namely, the choice of the model parameters that reproduce saturation properties on nuclear matter have been intensively discussed. In Ref. [36] the Kaplan-Nelson chiral Lagrangian has been used to describe the kaon-baryon sector while a Walecka-like Lagrangian was chosen for the baryon-baryon sector. However, as argued in Ref. [37], there is some lack of consistency that may influence the results. Using a meson-exchange model allows the simultaneous inclusion of baryons (nucleons and hyperons) and pions (kaons) and uses the same kind of interaction to describe the baryon-baryon and baryon-pion (kaon) interaction.

The Lagrangian density in the minimal coupling scheme [37–43] is given by

$$\mathcal{L}_b = D_\mu^*\Phi^*D^\mu\Phi - m_b^{*2}\Phi^*\Phi, \tag{18}$$

where the covariant derivative is

$$D_\mu = \partial_\mu + iX_\mu, \tag{19}$$

$$X_\mu \equiv g_{\omega b}\omega_\mu + g_{\rho b}\vec{\tau}_b\cdot\vec{\rho}_\mu, \tag{20}$$

and the boson effective mass $m_b^* = m_b - g_{\sigma b}\sigma$. The boson field can then represent either the kaons or pions (particles and antiparticles):

$$\Phi \equiv (K^+, K^0), \quad \Phi^* \equiv (K^-, \bar{K}^0), \tag{21}$$

or

$$\Phi \equiv (\pi^-, \pi^0), \quad \Phi^* \equiv (\pi^+, \pi^0). \tag{22}$$

The isospin third-component to the bosons is given by

$$\tau_{3\pi} = \begin{cases} +1, \pi^+; \\ 0, \pi^0; \\ -1, \pi^-; \end{cases} \qquad \tau_{3K} = \begin{cases} +\frac{1}{2}, & K^+, \bar{K}^0. \\ -\frac{1}{2}, & K^-, K^0. \end{cases} \tag{23}$$

We determine the thermodynamic potential within the mean-field approximation and perform a calculation similar to that carried out in Ref. [43] with the respective modifications in the covariant derivative (19).

For simplicity we have set $g_{\sigma\pi} = 0$, then $m_\pi^* = m_\pi$, and also $g_{\omega\pi} = 0$ such that the σ-π and ω-π interactions have been turned off. The neutral pion is its own antiparticle ($\tau_{30} = 0$), so in the mean-field approximation and taking into account

the above considerations, Eq. (20) becomes $X_\mu = 0$. Thus the π^0 EOS is that of a free boson gas at temperature T and zero chemical potential.

In the Appendix we show the calculation of the bosonic EOS:

$$P_b = \zeta^2\left[(\mu_b - X_0)^2 - m_b^{*2}\right] - T\int \frac{d^3p}{(2\pi)^3}\{\ln[1 - e^{-\beta(\omega^+ - \mu)}] + \ln[1 - e^{-\beta(\omega^- + \mu)}]\}, \tag{24}$$

$$\mathcal{E}_b = \zeta^2\left[m_b^{*2} + \left(\mu_b^2 - X_0^2\right)\right] + \int \frac{d^3p}{(2\pi)^3}\{\omega^+ f_{B+} + \omega^- f_{B-}\}, \tag{25}$$

$$n_b = 2\zeta^2(\mu_b - X_0) + \int \frac{d^3p}{(2\pi)^3}\{f_{B+} - f_{B-}\}, \tag{26}$$

where the Bose distribution for particles (f_{B+}) and antiparticles (f_{B-}) appears naturally in the EOS and reads

$$f_{B\pm} = \frac{1}{e^{\beta(\omega^\pm \mp \mu_b)} - 1} = \frac{1}{e^{\beta[(\epsilon_b^* \pm X_0) \mp \mu_b]} - 1} = \frac{1}{e^{\beta(\epsilon_b^* \mp \nu_b)} - 1}, \tag{27}$$

with $\epsilon_b^* = \sqrt{p^2 + m_b^{*2}}$, and hence we define the boson effective chemical potential as

$$\nu_b \equiv \mu_b - X_0. \tag{28}$$

From Eq. (26) one notes two contributions in the boson density and we can define them as the "condensate" and the "thermal" contribution,

$$n_b = n_b^c(\zeta) + n_b^T(T), \tag{29}$$

and the entropy density is given by $s_b = \beta(P_b + \mathcal{E}_b - \mu_b n_b)$. The order parameter ζ can be obtained through the minimization of the thermodynamic potential.

D. Hadron phase equations

The thermodynamic potential of the hadron phase (HP), including both the baryons and the bosons, is given by

$$\Omega_{\rm HP} = \Omega_B + \Omega_b, \tag{30}$$

where Ω_B is given by Eq. (12) and Ω_b by Eq. (A19). By minimizing the thermodynamic potential $\Omega_{\rm HP}$ with respect to the meson fields σ, ω, and ρ, and also with respect to the order parameter ζ, within the mean-field approximation ($\sigma \to \langle\sigma\rangle = \sigma_0; \omega_\mu \to \langle\omega_\mu\rangle = \delta_{\mu 0}\omega_0; \vec{\rho}_\mu \to \langle\vec{\rho}_\mu\rangle = \delta_{\mu 0}\delta^{i3}\rho_0^3 \equiv \delta_{\mu 0}\delta^{i3}\rho_{03}$), we obtain the equations for the hadron phase:

$$\begin{aligned} m_\sigma^2\sigma_0 &= -\frac{k}{2}\sigma_0^2 - \frac{\lambda}{6}\sigma_0^3 + \sum_j g_{\sigma j} n_j^s + \sum_b g_{\sigma b}\left(n_b^c + n_b^s\right), \\ m_\omega^2\omega_0 &= -\frac{\xi g_\omega^4}{6}\omega_0^3 + \sum_j g_{\omega j} n_j + \sum_b g_{\omega b} n_b \\ &\quad - 2\Lambda_{\rm v} g_\rho^2 g_\omega^2 \rho_{03}^2 \omega_0, \\ m_\rho^2\rho_{03} &= \sum_j g_{\rho j}\tau_{3j} n_j + \sum_b g_{\rho b}\tau_{3b} n_b - 2\Lambda_{\rm v} g_\rho^2 g_\omega^2 \omega_0^2 \rho_{03}, \end{aligned} \tag{31}$$

and

$$\zeta[\mu_b - \omega_b^+(0)][\mu_b + \omega_b^-(0)] = 0, \tag{32}$$

where

$$n_j^s = 2\int \frac{d^3p}{(2\pi)^3}\frac{m_j^*}{E_j^*}(f_{F+} + f_{F-}) \tag{33}$$

is the baryon scalar density of particle j, and the respective baryon density is

$$n_j = \frac{2}{(2\pi)^3}\int d^3p (f_{F+} - f_{F-}). \tag{34}$$

The "boson scalar density" for the boson b is given by

$$n_b^s = \int \frac{d^3p}{(2\pi)^3}\frac{m_b^*}{\epsilon_b^*}(f_{B+} + f_{B-}), \tag{35}$$

and the boson density is given by Eq. (26).

From the Eq. (32) we obtain the conditions for the possibility of a boson condensate ($\zeta = 0$, no condensate), resulting in

$$\mu_b = \omega_b^+(p = 0) \quad \text{or} \quad \mu_b = -\omega_b^-(p = 0), \tag{36}$$

depending on the signal of μ_b (either positive or negative). Thus

$$\mu_b = m_b^* + X_0 \quad \text{or} \quad \mu_b = -(m_b^* - X_0), \tag{37}$$

and

$$\mu_b - X_0 = m_b^* \quad \text{or} \quad \mu_b - X_0 = -m_b^*, \tag{38}$$

such that the condition for the onset of the condensate state is

$$\nu_b \to m_b^* \quad \text{or} \quad \nu_b \to -m_b^*. \tag{39}$$

According to Eqs. (24) and (39) the condensate (zero momentum state) does not contribute to the pressure of the system as expected. When the condensate is not present, $\zeta = 0$.

III. THE MIXED PHASE

In the following, three situations for the phase coexistence are discussed in detail: (A) hadron matter consisting of nucleons and quark matter consisting of quarks u and d; (B) hadron matter consisting of nucleons and pions and quark matter consisting of quarks u and d; and (C) hadron matter consisting of nucleons, hyperons, pions, and kaons with zero net strangeness and quark matter consisting of quarks u and d.

A. Nucleons and quarks

According to the Gibbs' conditions [24] for the phase coexistence, the chemical potentials, temperatures, and pressures have to be identical in both phases (H = hadron phase; Q = quark phase):

$$\begin{aligned} \mu_u^H &= \mu_u^Q, \\ \mu_d^H &= \mu_d^Q, \\ T^H &= T^Q, \\ P^H\left(\mu_u^H, \mu_d^H, T\right) &= P^Q\left(\mu_u^Q, \mu_d^Q, T\right). \end{aligned} \tag{40}$$

The conservation of the isospin (n_3) and baryon densities (n_B) is also required, so that in terms of these two charges [25] and including the mixed phase we can write

$$\begin{aligned} P^H\left(n_B^H, n_3^H, T\right) &= P^Q\left(n_B^Q, n_3^Q, T\right), \\ \mu_B^H\left(n_B^H, n_3^H, T\right) &= \mu_B^Q\left(n_B^Q, n_3^Q, T\right), \\ \mu_3^H\left(n_B^H, n_3^H, T\right) &= \mu_3^Q\left(n_B^Q, n_3^Q, T\right), \\ n_B &= (1-\chi)n_B^H + \chi n_B^Q, \\ n_3 &= (1-\chi)n_3^H + \chi n_3^Q, \end{aligned} \tag{41}$$

where for the hadron phase

$$\begin{aligned} n_B^H &= n_p + n_n, \quad n_3^H = \frac{n_p - n_n}{2}, \\ \mu_B^H &= \tfrac{1}{2}(\mu_p + \mu_n), \quad \mu_3^H = \mu_p - \mu_n, \end{aligned} \tag{42}$$

and for the quark phase

$$\begin{aligned} n_B^Q &= \tfrac{1}{3}(n_u + n_d), \quad n_3^Q = \frac{n_u - n_d}{2}, \\ \mu_B^Q &= \tfrac{3}{2}(\mu_u + \mu_d), \quad \mu_3^Q = \mu_u - \mu_d, \end{aligned} \tag{43}$$

and χ represents the fraction of quarks in the mixed phase. The asymmetry parameter α (isospin ratio) of the nuclei was defined as

$$\alpha \equiv \frac{N-Z}{N+Z} = \frac{n_n - n_p}{n_B}, \tag{44}$$

and the asymmetry parameter of the hadron and quark phases can be defined by

$$\alpha^H \equiv -2\frac{n_3^H}{n_B^H}, \quad \alpha^Q \equiv -2\frac{n_3^Q}{n_B^Q}, \tag{45}$$

hence

$$\alpha^H = \frac{n_n - n_p}{n_n + n_p}, \quad \alpha^Q = 3\frac{n_d - n_u}{n_d + n_u}, \tag{46}$$

such that $0 \leqslant \alpha^H \leqslant 1$ (just nucleons case) and $0 \leqslant \alpha^Q \leqslant 3$ (the quark case).

B. Nucleons, pions, and quarks

When bosons are present the isospin density of the hadron phase is modified according to Eq. (32) and α^H can be greater than 1. The isospin density of the hadron phase with π^- becomes

$$n_3^H = \frac{n_p - n_n}{2} - n_\pi, \tag{47}$$

where $n_\pi = n_\pi^c + n_\pi^T$ and we assume $g_{\rho N} = g_\rho = g_\pi$. In order to obtain the simplest thermodynamic features for the pions we set $g_{\omega\pi} = 0$ and for simplicity we set $g_{\sigma\pi} = 0$, so that in this case $m_\pi^* = m_\pi$. The in-medium (s wave) Bose effective pion energy is

$$\omega_{\pi^-}(p=0) = m_\pi - g_\rho \rho_{03}, \tag{48}$$

and the pion chemical potentials and the effective π^- chemical potential are

$$\mu_{\pi^-} = \mu_n - \mu_p, \quad \mu_{\pi^+} = -\mu_{\pi^-}, \tag{49}$$

$$\mu_{\pi^0} = 0, \quad \nu_{\pi^-} = \mu_{\pi^-} + g_\rho \rho_{03}. \tag{50}$$

Because $\mu_n > \mu_p$, then $\mu_{\pi^-} > 0$, and according to Eq. (39) the onset of the pion (π^-) condensation takes place when

$$\nu_{\pi^-} \to m_\pi. \tag{51}$$

The EOS for the hadronic phase are

$$P_H = P_B + P_\pi + P_{\pi^0}, \quad \mathcal{E}_H = \mathcal{E}_B + \mathcal{E}_\pi + \mathcal{E}_{\pi^0}, \tag{52}$$

where P_π and $\mathcal{E}_\pi$ are given by Eqs. (24) and (25) and we have also included the neutral pions as a free Bose gas.

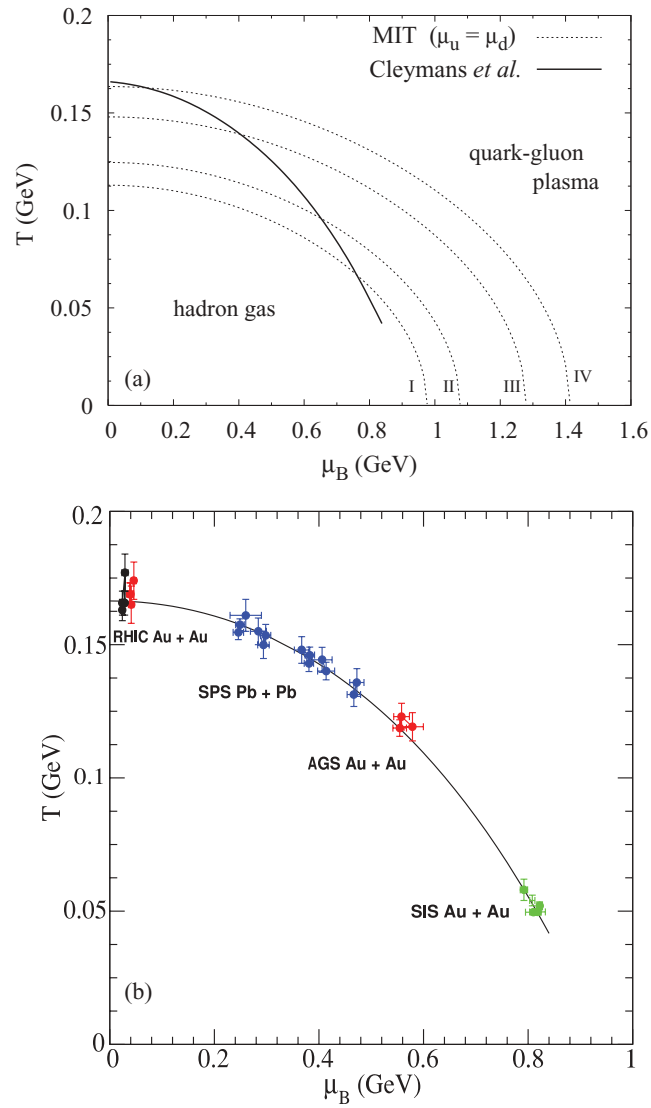

FIG. 1. (Color online) (a) A simple qualitative overview on the T × μ_B curve in the MIT bag model (dashed curves) for the case $\mu_u = \mu_d$, compared with the freeze-out curve (continuous line) from panel (b). The bag constant values from I to IV are $B^{1/4} = 145$, 160, 190, and 210 MeV. (b) A parametrization of the freeze-out curve deduced from particle multiplicities in heavy-ion collisions (Cleymans *et al.* [44]).

TABLE III. Parameter sets used in this work and corresponding saturation properties.

	FSU [49]	TM1 [47]	TM1$\omega\rho$ [48]	NLρ [51]	NL3 [46]	GM1 [50]	GM3 [50]
n_0 (fm^{-3})	0.148	0.145	0.145	0.160	0.148	0.153	0.153
K (MeV)	230	281	281	240	271.76	300	240
m^*/m	0.62	0.643	0.643	0.75	0.60	0.70	0.78
m (MeV)	939	938	938	939	939	938	938
$-B/A$ (MeV)	16.3	16.3	16.3	16.0	16.299	16.3	16.3
$\mathcal{E}_{\rm sym}$ (MeV)	32.6	36.9	31.9	30.5	37.4	32.5	32.5
L (MeV)	61	110	55	85	118	94	90
m_σ (MeV)	491.5	511.198	511.198	512	508.194	512	512
m_ω (MeV)	782.5	783	783	783	783	783	783
m_ρ (MeV)	763	770	770	763	763	770	770
g_σ	10.592	10.029	10.029	8.340	10.217	8.910	8.175
g_ω	14.302	12.614	12.614	9.238	12.868	10.610	8.712
g_ρ	11.767	9.264	11.147	7.538	8.948	8.196	8.259
b	0.000756	−0.001506	−0.001506	0.006935	0.002052	0.002947	0.008659
c	0.003960	0.000061	0.000061	−0.004800	−0.002651	−0.001070	−0.002421
ξ	0.06	0.0169	0.0169	0	0	0	0
$\Lambda_{\rm v}$	0.03	0	0.03	0	0	0	0

C. The baryon octet, pions, kaons, and quarks

At this stage we have included in the hadron phase all baryons of the baryon octet and to keep the strangeness conservation as $\sum_i S_i = 0$ in both phases we also have included the K^+ meson in the hadron phase. For the Gibbs' conditions (40) we need to add $\mu_s^H = \mu_s^Q$, so that we can write the chemical potential as $\mu_i = B_i\mu_B + I_{3i}\mu_3 + S_i\mu_S$, where B_i, I_{3i}, and S_i are the baryonic, isospin, and strangeness quantum numbers of particle i.

The equations for the baryons and bosons are already presented in this work. For the kaons we set $g_{\rho K} = g_\rho$, $g_{\omega K} = 0$, and also $g_{\sigma K} = 0$, such that $m_K^* = m_K$ as for the pions. We are aware that this choice is very naive. It was done to explore the isospin degree of freedom. In a future work a more realistic parametrization of the kaon-meson coupling will be used which will allow us to discuss the strangeness degree of freedom more completely.

IV. RESULTS

First of all it is important to present some features of the MIT bag model. Figure 1 shows a qualitative overview of the MIT bag model in a simple case when $\mu_u = \mu_d$, in comparison with data analysis of some collision experiments [44]. This figure also indicates the best values of the bag constant B to be used in some energy ranges that we describe in the present work. At high temperatures and low baryon chemical potential (low density) we use the values $B^{1/4} = 190$ and 210 MeV. On the other hand, our analysis at intermediate energies is performed with $B^{1/4} = 160$ MeV.

For the hadronic phase we use the parameter sets presented in Table III, where we give the symmetric nuclear matter properties at saturation density as well as the parameters of the models. In Figs. 2(a) and 2(b) the pressure of the symmetric nuclear matter and the symmetry energy, respectively, are plotted for a large range of densities. In Fig. 2(a) we also

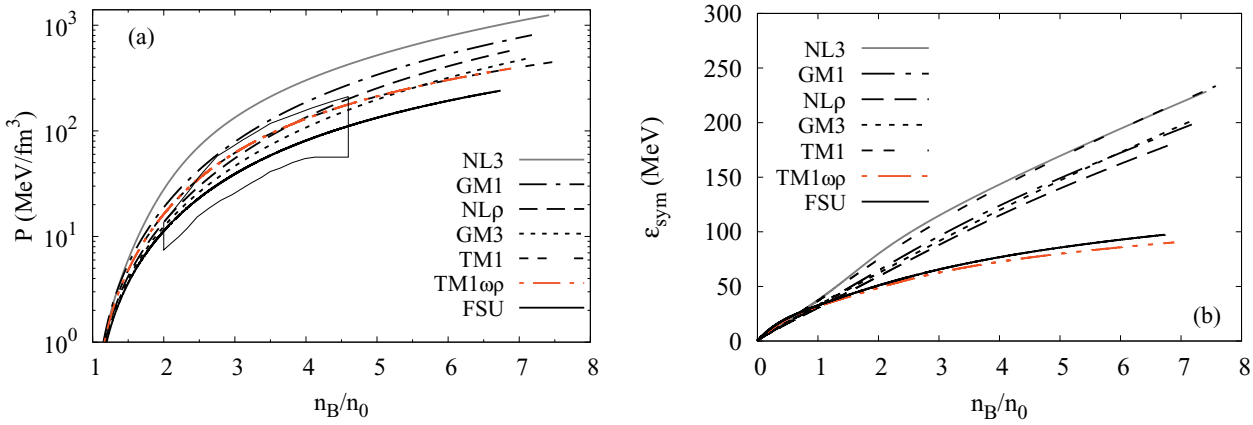

FIG. 2. (Color online) EOS for symmetric matter and different models. (a) Pressure as a function of the baryon number density. The enclosed area represents experimental data according to Ref. [45]. (b) The symmetry energy as a function of the baryon number density.

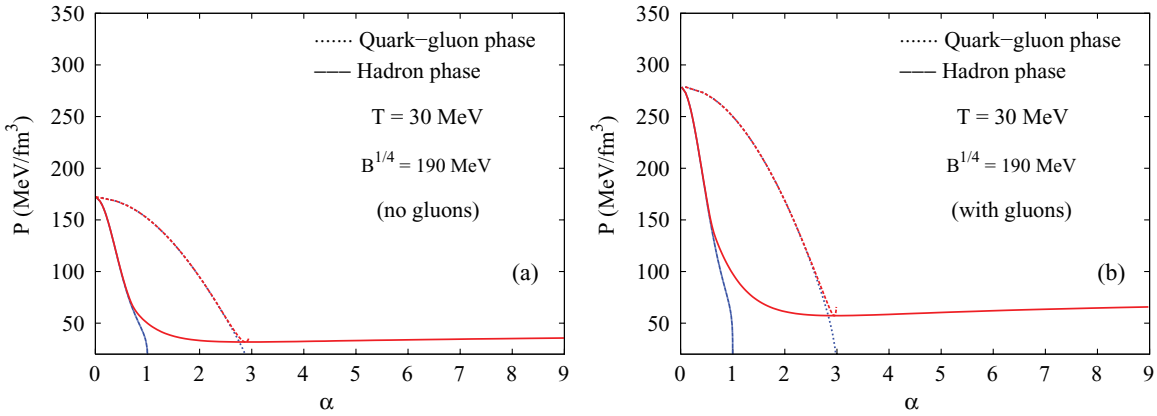

FIG. 3. (Color online) Binodal sections at $T = 30$ MeV and the effect of pions and gluons. The NL3 parameter set is used. The blue lines indicate a system with no pions. The red ones indicate the presence of pions. (a) Without gluons. (b) With gluons.

include the experimental constraints obtained from collective flow data in heavy-ion collisions [45]. We have considered a wide range of models frequently used to study stellar matter or finite nuclei. Even though some of them do not satisfy the constraints determined in Ref. [45], as a whole these sets of models allow us to understand the influence of a hard/soft EOS and a hard/soft symmetry energy of the hadron-matter–quark-matter phase transition. We have considered NL3 [46], with a quite large symmetry energy and incompressibility at saturation and which was fitted in order to reproduce the ground-state properties of both stable and unstable nuclei; TM1 [47], which also reproduces the ground-state properties of both stable and unstable nuclei and provides an equation of state of nuclear matter similar to the one obtained in the RBHF (relativistic Brueckner-Hartree-Fock) theory, softer than NL3 at high densities; TM1$\omega\rho$ [48]; the TM1 parametrization with a mixed isoscalar-isovector coupling which we fix in order to obtain a softer density dependence of the symmetry energy [34]; FSU [49], which was accurately calibrated to simultaneously describe the GMR in ^{90}Zr and ^{208}Pb and the IVGDR in ^{208}Pb and still reproduce ground-state observables of stable and unstable nuclei; GM1 and GM3 [50], generally used to describe stellar matter, with a symmetry energy not so hard as the one of NL3 and TM1; and NLρ [51], which has been used to discuss the hadron-matter–quark-matter transition in Ref. [28] and which presents an EOS at high densities between GM1 and GM3.

Let us first describe some hadron-quark matter systems at zero and finite temperature, including the deconfined phase transition, through isothermal processes. We first discuss the effects of pions and gluons on the phase transition. For this discussion we take NL3 to describe the hadronic matter; however, the main conclusions do not depend on the nuclear model considered.

In Figs. 3(a) and 3(b) we show slices of the binodal surface indicating the two-dimensional phase-coexistence boundary in the $\{P, T, \alpha\}$ space, at $T = 30$ MeV. For each temperature, the binodal section is divided into two branches. One branch describes the system in the hadron phase, while the other branch describes the quark-gluon phase. In both figures the role of the pions and gluons is presented. Figure 3(a) shows a system with no gluons for two cases with and without the pions. The blue curves represent a system with no pions. The gluons have a very strong effect on the critical point, corresponding to a maximum in the pressure, when both phases coexist for $\alpha = 0$. The presence of gluons increases the critical pressure almost by 100%. The role of the pions is better seen in Fig. 3(b) (red lines). The asymmetry parameter of the hadron phase increases due to the presence of the pions which increase the isospin interaction. In equilibrium, the pressures in both phases must be equal according to the Gibbs' conditions. When pions are present these conditions still hold. We observe a slight increase of the pressure of the quark-gluon phase for $\alpha > 3$, following the hadronic pressure increase.

At finite temperature pions are present as a Bose gas and their presence as a condensate state at low enough temperatures is also possible. The presence of a pion gas and a pion condensate changes the pressure at low densities according to Fig. 4 by increasing the absolute value of the ρ meson field (i.e., the isospin interaction) because the condensate itself does not contribute to the pressure of the system as a boson gas. The lowest pressures of the binodal section occur for the largest

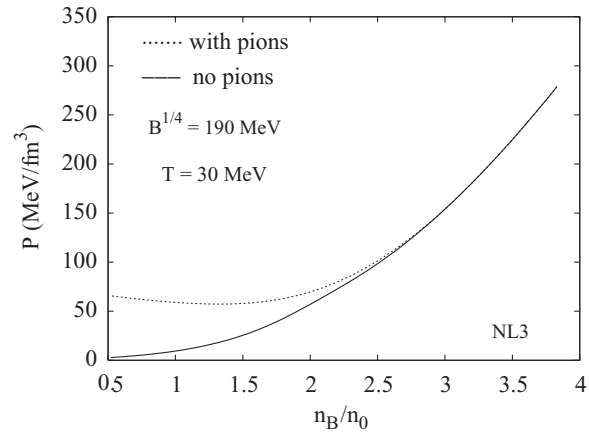

FIG. 4. Binodal section: Pressure as a function of the baryonic density. The presence of the pions increases the isospin interaction such that a pressure increase is observed.

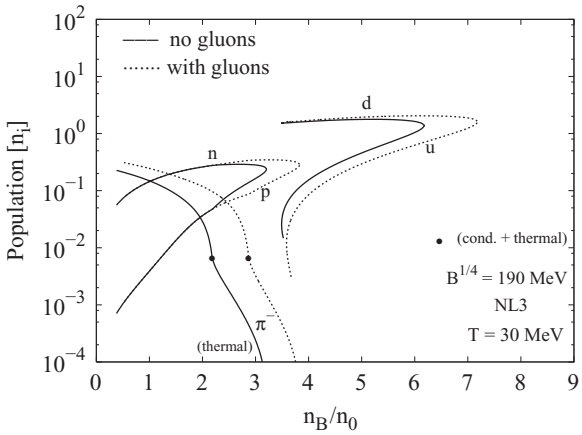

FIG. 5. Population of particles at $T = 30$ MeV with and without the gluons. The solid circles mark the onset of the pion condensate at $2.18n_0$ in the first case and at $2.87n_0$ in the second one.

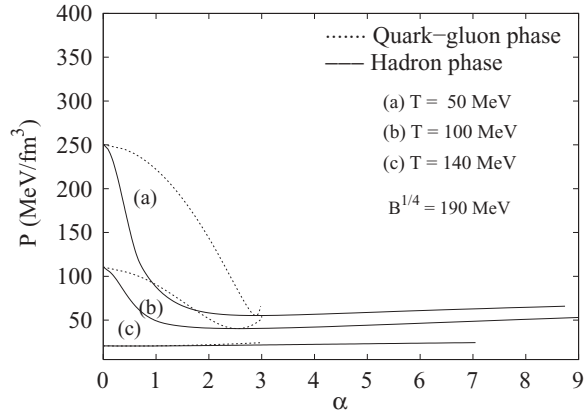

FIG. 7. Slices of the binodal surface using the NL3 parameter set and $B^{1/4} = 190$ MeV. The critical temperature is $T_c \sim 150$ MeV. The calculation includes both pions and gluons.

values of the asymmetry parameter α (1 for the hadronic phase without pions).

When gluons are included in the quark phase the densities reached by the system at the binodal surface increase slightly in both phases such that the onset of the pion condensation takes place at a slightly higher density: $2.87n_0$ instead of $2.18n_0$ at $T = 30$ MeV according to Fig. 5, when an isothermal process is analyzed. Therefore, the presence of gluons shifts the phase transition to a quark-gluon plasma to larger densities.

The onset of the pion condensation according to Eq. (39) [or similarly Eq. (36)] is clearly seen in Fig. 6 where we plot the pion mass m_π, the pion chemical potential μ_π, the pion effective chemical potential ν_π, and the pion frequency at $p = 0$, $\omega_b^+(p = 0)$. The pion condensation occurs for the lower densities when the conditions (39) or (36) are satisfied.

In Fig. 7 we show the binodal slices at different temperatures and for the bag constant 190 MeV. The enclosed area becomes smaller with increasing temperature and the pressure at $\alpha = 0$ decreases when the temperature increases. The two

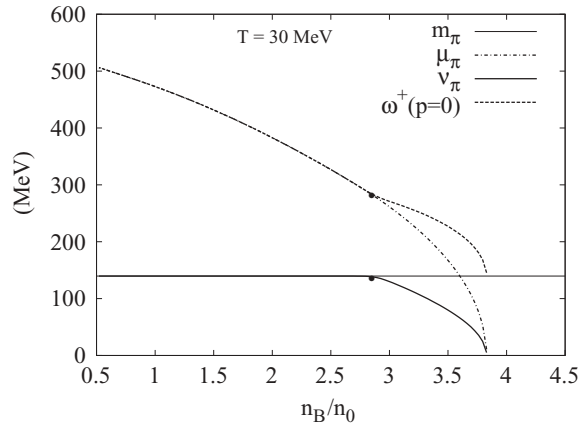

FIG. 6. The onset of the pion condensation for the case with gluons in Fig. 5. On the y axis we plot the pion mass, the chemical potential, the effective chemical potential, and the frequency at $p = 0$.

branches merge into a single line when the system reaches the critical temperature at zero chemical potential and density. The critical temperature (T_c) of the phase transition is ∼150 MeV for the bag constant $B^{1/4} = 190$ MeV. For larger values of B we obtain larger pressures at the same temperature and the other way round for smaller values. The results shown in the figure are consistent with the ones found in Ref. [26] although here the NL3 parameter set has been used. The calculation includes both pions and gluons.

Next we discuss the inclusion of strangeness. The population of particles at $T = 50$ MeV can be seen in Fig. 8 for two cases: (a) a simple system of protons, p, neutrons, n, and pions, π^-, in the hadron phase, and (b) including the hyperons of the baryon octet and K^+ mesons in the hadron phase. In both cases the total strangeness of the system is zero; therefore, we just have quarks u and d in the quark phase. Figure 8(a) shows an increase of pions at low baryon densities, which plays an important role in the isospin density of the system. Most of the pions below $2.6n_0$ are in a zero momentum state (i.e., a pion condensate). The same pattern can be seen in Fig. 8(b) on pions and nucleons, indicating that strange particles are not important under these conditions at that temperature but they do appear at higher densities. We do not see kaon condensation, just a pion condensate as in the first case. It is important to analyze how sensitive are the above results to the choice of the kaon-meson interaction. Work in this direction will be done in the near future.

We now discuss the effect of the density dependence of the EOS on the binodal surfaces. In Fig. 9(a) one sees a comparison of the hadron-phase–quark-phase binodal sections among the different parameter sets listed in Table III for the zero temperature case and $B^{1/4} = 160$ MeV. Qualitatively all the curves behave in the same way. The difference lies in the pressures and the densities reached by the different systems, which are explicitly shown in Fig. 9(b). We conclude that the different behaviors seen for the binodal sections are due to the EOS at large densities; see Fig. 2(a) where the pressure is plotted as a function of density for cold symmetric nuclear matter. At finite temperature a similar trend is obtained except that the maximum densities reached are smaller.

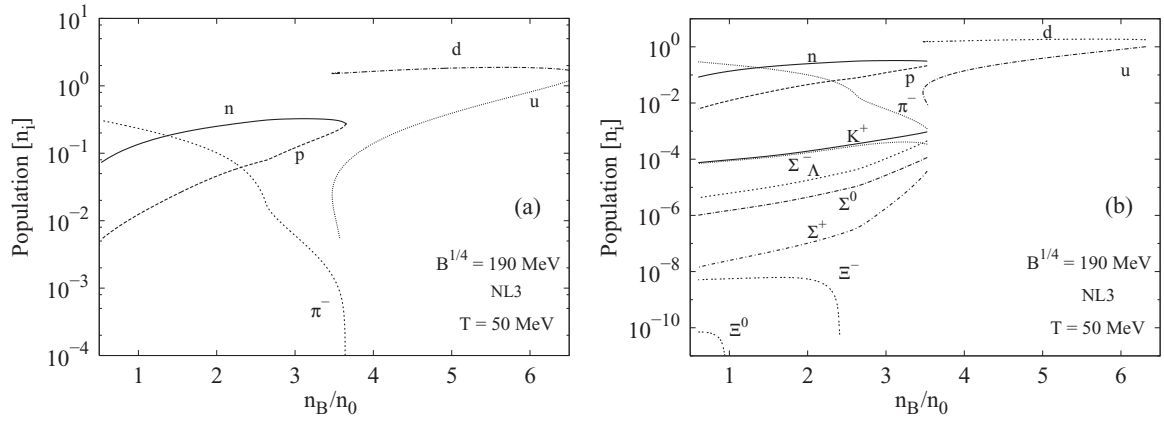

FIG. 8. Population of particles for the case in Fig. 7(a) at $T = 50$ MeV. (a) Just p, n, and π^- in the hadronic phase. (b) The baryon octet, π^-, and K^+ in the hadronic phase.

The effect of the symmetry energy on the binodal is better discussed analyzing Fig. 10 where the binodal for TM1 and TM1$\omega\rho$ is plotted without pions. These two models have the same isoscalar behavior and just differ in the isovector channel, TM1$\omega\rho$ having a softer symmetry energy. We conclude that a softer symmetry energy favors a phase transition at larger asymmetries. For the same reason the models with a softer symmetry energy have their binodals for larger asymmetries in Fig. 9(a).

Figures 2(a) and 2(b) are used in the following to discuss the differences between the models. We see that the hadron density at the binodal surface is very sensitive to the softness/hardness of the EOS at intermediate/high densities. In particular, the largest pressures are attained by the softest EOS. It is interesting to analyze the behavior of TM1: it behaves at low densities as a hard EOS like NL3 and at high densities as a soft one, giving the largest pressure at the critical point. It is the relative change of hard/soft character of the EOS that explains the crossing between the different models in Fig. 9(a). We have not included a curve for FSU because due to its softness no phase transition was obtained at reasonable densities. The behavior at large densities can be adjusted by changing the value of the parameter χ, which multiplies the forth power of the ω-meson term in the Lagrangian density. A larger value gives a softer EOS at large densities. We have reduced the value of χ and for $\chi = 0.03$ we could get convergence at reasonable densities. This coincides with the large density behavior of the new parametrization proposed in Ref. [52], which corrects the behavior of FSU at large densities, which predicted too small maximum star masses and too large star radii.

The density dependence of the energy density does not affect the binodal surface of symmetric nuclear matter but it certainly has an effect if we consider asymmetric matter. We investigate the phase transition at intermediate energies using a convenient choice of different parametrizations of the NLWM to explore different compressibilities at large densities as well as an asysoft and asyhard EOS. We take into account the following parameter sets: NL3, hard EOS and symmetry energy; NLρ, intermediate behavior in both the isoscalar and the isovector channel; TM1, soft EOS at high densities and hard symmetry energy; and TM1$\omega\rho$, with a soft symmetry energy.

To discuss the effect of isospin asymmetry on the binodal sections, we allow the temperature to change with fixed

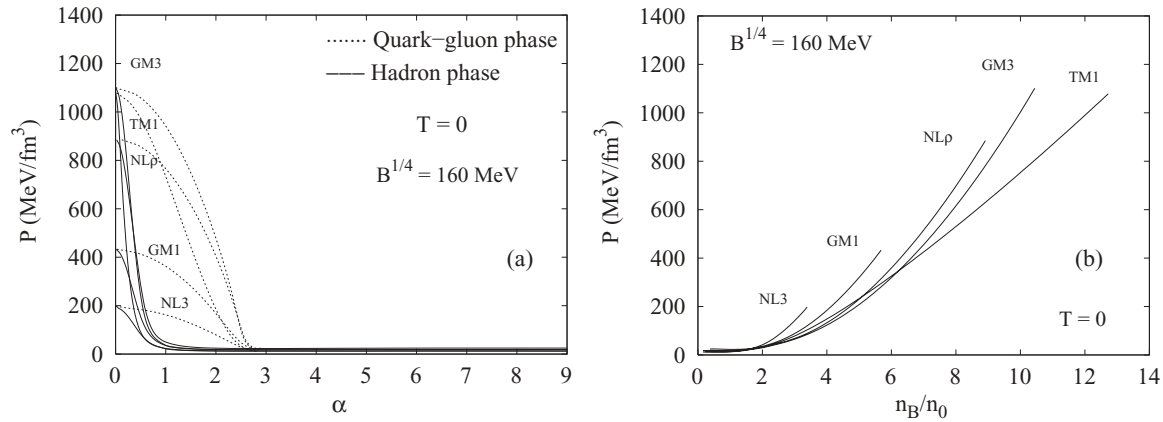

FIG. 9. (a) Pressure as a function of the asymmetry parameter for different parametrizations at zero temperature. (b) Pressure as a function of the baryon number density for the case in panel (a).

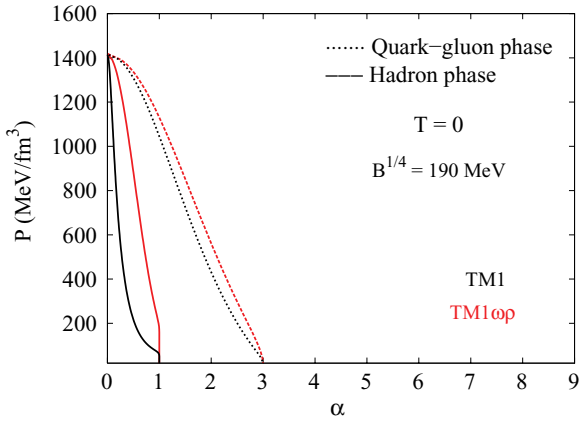

FIG. 10. (Color online) The effect of the ω-ρ coupling on the binodal at $T = 0$.

asymmetry parameter and compare the predictions of the different models. Figures 11(a) and 11(b) show, for NL3 and NLρ, the binodal sections in the $\{n_B, T, \alpha\}$ space and the projection of several branches at different α onto the (n_B, T) plane (HP = hadron phase; QP = quark phase). In other words Figs. 11(a) and 11(b) show the QCD phase diagram with different asymmetries, $\alpha = 0$, 0.2, 0.4, 0.6, 0.8, and 1.0, from the right (I) to the left (II) in the two phases. From now on, in order not to reach too high densities in the hadron phase we exclude the gluons from the system. This does not affect the comparison between models and may give rise to a maximum 20% underestimation of the transition density.

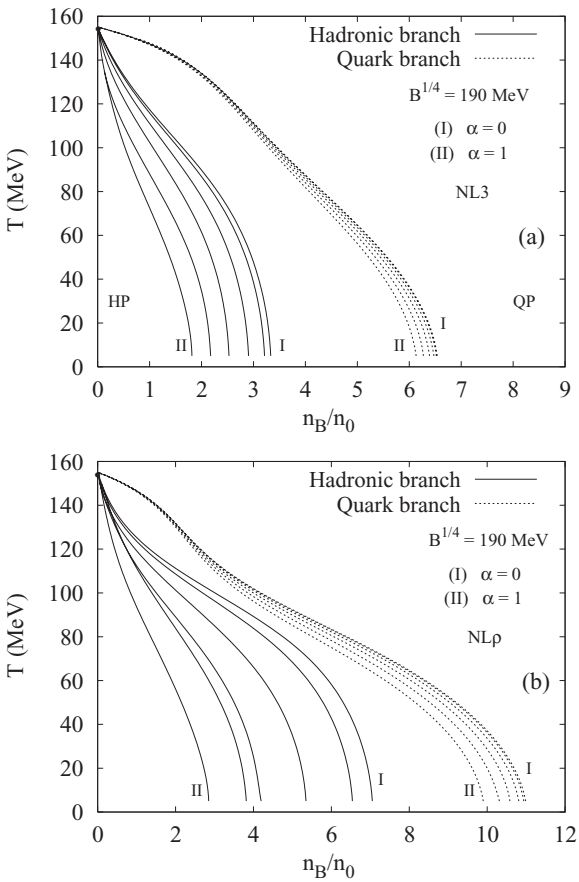

FIG. 11. (a) Binodal section in the (n_B, T, α) space and the projection of several branches for different asymmetry parameter α onto the (n_B, T) plane. The asymmetries are $\alpha = 0$, 0.2, 0.4, 0.6, 0.8, and 1.0, from the right (I) to the left (II) in the two phases, with no gluons. (b) Same as panel (a) for the NLρ parameter set. In both cases the critical temperature where $\mu_B = 0$ is $T_c \sim 155$ MeV.

In Fig. 11(a) we have considered $B^{1/4} = 190$ MeV together with the models NL3 and NLρ. The properties of the EOS are clearly reflected on these results: for NL3 the transition occurs for smaller densities due to its very large compressibility at large densities. It is also this high value of the compressibility that dilutes in part the effect of the asymmetry parameter. NLρ has a much softer EOS and symmetry energy and, therefore, the curves obtained for a fixed asymmetry span a larger range of densities. In summary, the hadron-quark phase transition is favored when the asymmetry of the system is increased.

We are interested in discussing the phase transition at intermediate temperatures and high densities and, for this reason, we consider smaller bag pressures according to Fig. 1. We set $B^{1/4} = 160$ MeV to reach a specific range of temperature and densities, which is presented in Figs. 12(a) and 12(c) and also in Fig. 13(a). The asymmetries experimentally available up to now according to Table II are in the range 0–0.23.

Since NL3 is too hard and does not satisfy most of the constraints imposed by experimental and observational measurements [53] we consider in the following TM1 with and without a $\omega\rho$ nonlinear term that allows us to discuss a asy-soft and a asy-hard EOS. We also take into account the NLρ parametrization in order to compare with the results already obtained in Ref. [27].

In Fig. 12 we compare TM1 and TM1-$\omega\rho$. This allows us to discuss the effect of density dependence of the symmetry energy on the phase transition because the isoscalar channel is kept fixed. The main effect of a softer symmetry energy is to shift the binodal sections for larger values of the asymmetry parameter to larger densities. A harder symmetry energy allows the occurrence of the hadron-quark phase transition at smaller densities and, therefore, is easier to reach with heavy-ion collisions at intermediate energies. Similar conclusions were drawn in Ref. [28] where the effect of the δ meson on the phase transition was discussed: the δ meson gives rise to a harder symmetry energy at large densities favoring the hadron-quark phase transition.

In Fig. 13(a) we show for the same bag constant the binodal sections obtained with NLρ. It is seen that due to a softer EOS at intermediate densities the binodal sections occur at larger densities when compared with TM1. The effect of the bag constant is clear if we compare Fig. 11(b) with $B^{1/4} =$ 190 MeV with Fig. 13(a). A larger B shifts the phase transition to much larger densities, showing that in order to obtain a good estimation it is essential to choose an adequate value of B.

We show in Figs. 12(b) and 12(d) and Fig. 13(b) a part of Figs. 12(a) and 12(c) and also Fig. 13(a), corresponding to $\alpha = 0.2$. We also include curves corresponding to the mixed phase with the quark concentrations $\chi = 0.2$ and 0.5 which

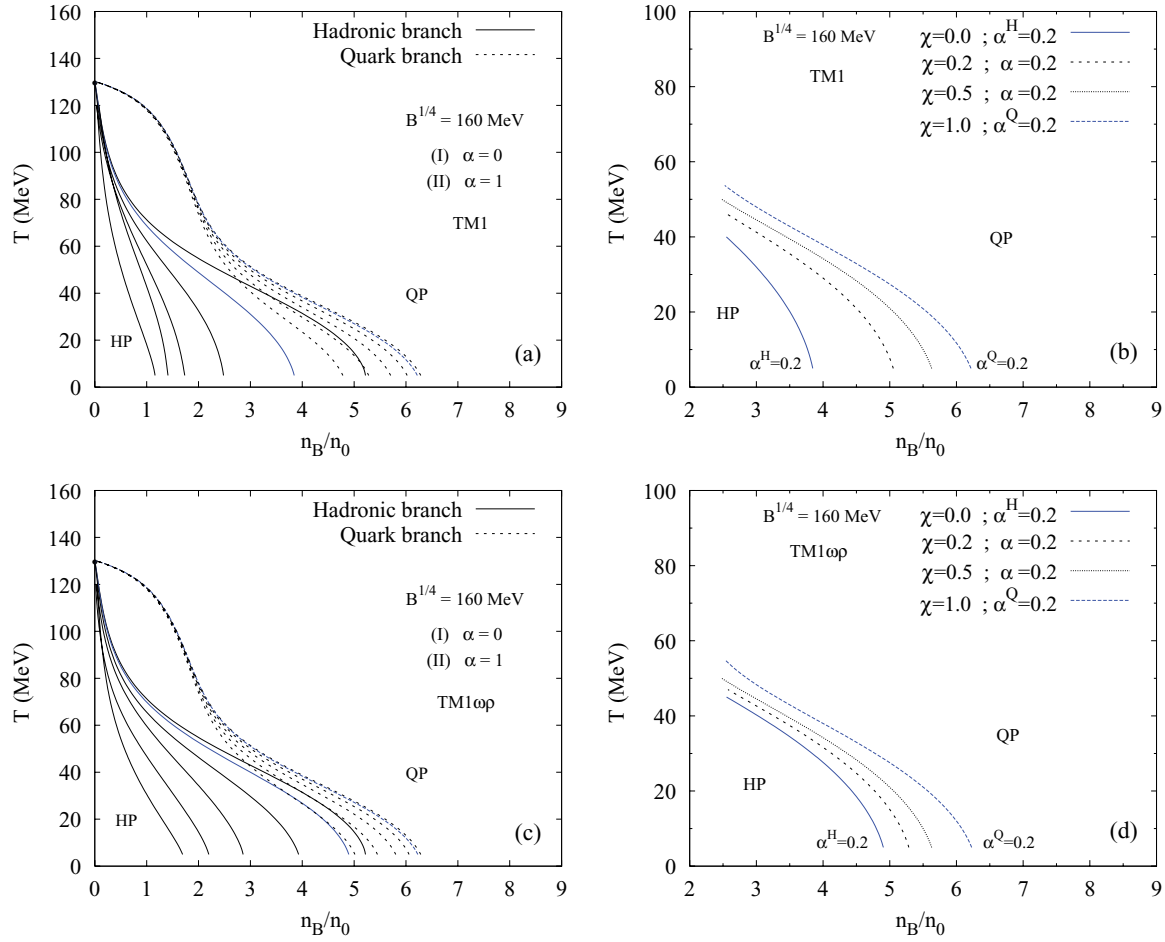

FIG. 12. (Color online) Same as in Fig. 11 for $B^{1/4} = 160$ MeV. The critical temperatures are $T_c \sim 130$ MeV and the labels (I) and (II) also represent the asymmetry in the same way as in Fig. 11. (a) The TM1 parameter set is used. (b) Part of Fig. 12(a) for $\alpha = 0.2$ with the mixed phase for different quark concentrations ($\chi = 0.2, 0.5$). (c) The TM1 parameter set and the mixing term Λ_v have been used in the present case. (d) Part of Fig. 12(c) with the mixed phase.

correspond to 20% and 50% of quarks in the mixed phase. One sees the indication of an interesting region where the phase transition probably occurs and can be probed by intermediate-energy heavy-ion collisions. This region is located in the range $n_B = 2 - 4n_0$ and $T = 50$–65 MeV and can reached by the new planned facilities (NICA) at JINR/ Dubna [19] and (FAIR)

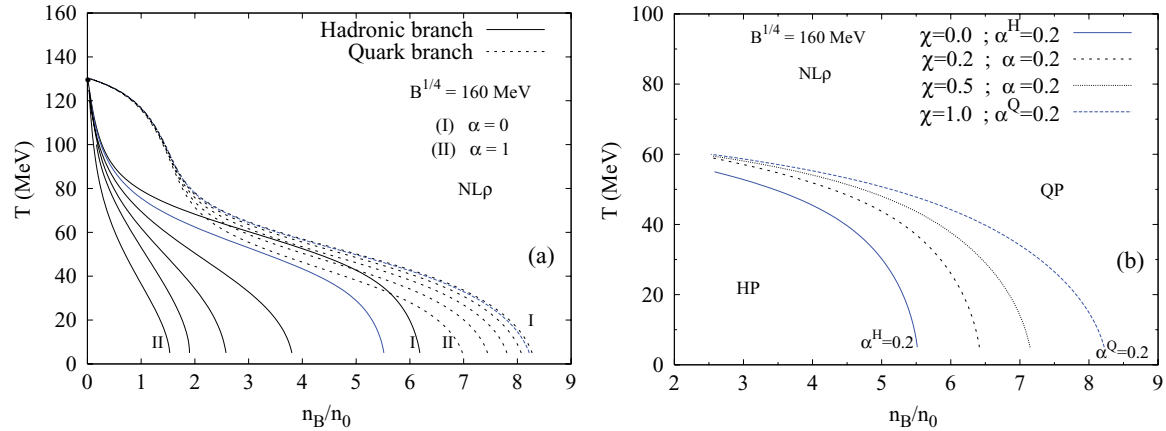

FIG. 13. (Color online) (a) Same as in Fig. 11(b) for $B^{1/4} = 160$ MeV. (b) Part of Fig. 13(a) for $\alpha = 0.2$ with the mixed phase for different quark concentrations ($\chi = 0.2, 0.5$).

at GSI/Darmstadt [20] that will start operations in the next few years.

The density behavior at intermediate/high densities defines the transition region. For instance, models TM1 and TM1$\omega\rho$ would favor the detection of a quark phase more than NLρ.

V. SUMMARY

We have presented a study of the deconfinement phase transition from hadronic matter to a quark-gluon plasma that could be formed in heavy-ion collisions. Calculations at finite temperature with a simple two-phase model and the inclusion of pion and kaon condensation were done to describe this type of system. We have studied the effect of the density dependence of the EOS on the phase transition choosing a convenient set of parametrizations of the NLWM. We have considered both hard and soft EOS at intermediate densities as well as models with asyhard and asysoft symmetry energies. We have also considered the effect of gluons on the quark phase. For the quark phase we have used the MIT bag model and chose the bag constant according to a parametrization of the freeze-out curve deduced from particle multiplicities in heavy-ion collisions [16]: for deconfinement phase transition at $T \sim 50$–60 and $\rho \sim 2$–$6\rho_0$, the bag constant $B^{1/4} \sim 160$ MeV was used.

An important result is the difference between the phase diagram for a symmetric system and that for asymmetric matter as observed in liquid-gas phase transition. Usually, the onset of the phase transition takes place at lower baryon densities and temperatures in more asymmetric systems. This can be probed by means of neutron-rich nuclei in heavy-ion collisions. Moreover, the density at which the phase transition occurs is sensitive to the density dependence of the EOS at intermediate densities. A hard EOS gives rise to a transition at lower densities. The density dependence of the symmetry energy also affects the transition when asymmetric matter is considered. The phase transition is favored for asymmetric nuclear matter and even more for an asyhard symmetry energy.

Both thermal pions and pion condensation have been included in the calculation. They mainly play a role at low densities, large isospin asymmetries, and large temperatures. We have considered that the pions couple to the nucleons through the ρ meson [26]. Using an equivalent parametrization for the kaon-meson coupling, which maybe too naive because it only takes into account the isospin interaction, we have verified that the effect of including strangeness in the hadron phase was negligible for a system with an overall strangeness equal to zero. This can be generalized to finite strangeness when it becomes possible to prepare heavy-ion collisions with hypernuclei. It remains to be investigated how sensitive are the results to the pion and kaon interaction.

The results obtained for the phase transition are very sensitive to the EOS. Both the isoscalar and the isovector interactions have an effect on the transition density. According to the effective models used in this work there exists a region in the parameter space where the phase transition probably occurs and can be probed by heavy-ion collisions at intermediate energies. This region is located in the range $n_B = 2$–$4n_0$ and $T = 30$–65 MeV and can be reached by the new planned facilities (NICA) at JINR/ Dubna [19] and (FAIR) at GSI/Darmstadt [20] that will start operations in the next few years. We have obtained a larger T interval, extending to lower temperatures, for the same densities obtained in Ref. [28] due to the properties of the models used. A clear sign of a phase transition could be used to constrain both the EOS and the symmetry energy at intermediate densities.

We have verified that models with a soft EOS and soft symmetry energy such as FSU do not predict a hadron-quark phase transition at densities that could be attained in the laboratory.

A more complete system with all baryons of the baryonic octet and strange mesons, as well as interacting pions and kaons, and using interactions constrained by experimental measurements is under investigation in order to get more systematic results.

ACKNOWLEDGMENTS

This work was partially supported by the CNPq (Brazil) and CAPES (Brazil)/FCT (Portugal) under Project 232/09 and by the FCT (Portugal) under the Grants PTDC/FIS/64707/2006 and CERN/FP/109316/2009. R.C. is grateful for the warm hospitality at the Centro de Física Computacional/FCTUC.

APPENDIX: THE BOSON THERMODYNAMIC POTENTIAL

Using the Lagrangian density in the minimal coupling scheme [37–43]

$$\mathcal{L}_b = D_\mu^* \Phi^* D^\mu \Phi - m_b^{*2} \Phi^* \Phi, \tag{A1}$$

it is possible to obtain the respective thermodynamic potential and the EOS of the boson fields. It is convenient to transform Φ into real and imaginary parts using two real fields, $\phi_1(\mathbf{x}, t)$ and $\phi_2(\mathbf{x}, t)$, such that

$$\Phi = \frac{1}{\sqrt{2}}(\phi_1 + i\phi_2), \quad \Phi^* = \frac{1}{\sqrt{2}}(\phi_1 - i\phi_2). \tag{A2}$$

The conjugate momenta are

$$\begin{aligned} \pi_1 &= \frac{\partial \mathcal{L}_b}{\partial(\partial_0 \phi_1)} = \partial_0 \phi_1 - X_0 \phi_2, \\ \pi_2 &= \frac{\partial \mathcal{L}_b}{\partial(\partial_0 \phi_2)} = \partial_0 \phi_2 + X_0 \phi_1, \end{aligned} \tag{A3}$$

and the corresponding Hamiltonian density of the boson field is $\mathcal{H}_b = \pi_1 \partial_0 \phi_1 + \pi_2 \partial_0 \phi_2 - \mathcal{L}_b$ such that the four-current and its zero component are

$$j_\mu = i[\Phi^*(D_\mu \Phi) - (D_\mu^* \Phi^*)\Phi], \tag{A4}$$

$$j_0 = \phi_2 \pi_1 - \phi_1 \pi_2. \tag{A5}$$

For the neutral pions we just have $\pi = \frac{\partial \mathcal{L}_b}{\partial(\partial_0 \phi)} = \partial_0 \phi$ and $\Phi = \frac{\phi}{2^{1/2}}$, such that $\Phi^* = \Phi$ and $j_\mu = 0$. Now we can write the

Hamiltonian density

$$\mathcal{H}_b = \frac{1}{2}\pi_1^2 + \frac{1}{2}\pi_2^2 + \pi_1(X_0\phi_2) - \pi_2(X_0\phi_1) + \frac{1}{2}(\vec{\nabla}\phi_1)^2 + \frac{1}{2}(\vec{\nabla}\phi_2)^2 + (\partial_i\phi_2)X_i\phi_1 - (\partial_i\phi_1)X_i\phi_2 + \frac{1}{2}(X_i\phi_1)^2 + \frac{1}{2}(X_i\phi_2)^2 + \frac{m_b^{*2}}{2}\left(\phi_1^2+\phi_2^2\right), \quad \text{(A6)}$$

where $i = 1, 2, 3$, and the partition function in the grand canonical ensemble as a functional integral is given by

$$Z_b = \int [d\pi_1][d\pi_2] \int_{\text{periodic}} [d\phi_1][d\phi_2] \exp\left\{\int_0^\beta d\tau \int d^3x \times \left[i\pi_1\frac{\partial\phi_1}{\partial\tau} + i\pi_2\frac{\partial\phi_2}{\partial\tau} - \mathcal{H}_b + \mu_b(\phi_2\pi_1 - \phi_1\pi_2)\right]\right\}, \quad \text{(A7)}$$

where μ_b is the boson chemical potential associated with the conserved charge $Q = \int d^3x j_0(x)$. Here "periodic" means that the integration over the field is constrained in the imaginary time variable $\tau = it$ so that $\phi_k(\mathbf{x}, 0) = \phi_k(\mathbf{x}, \beta)$, and where $\beta = 1/T$. The neutral pion Hamiltonian is $\mathcal{H}_{\pi^0} = \frac{1}{2}\pi^2 + \frac{1}{2}(\vec{\nabla}\phi)^2 + \frac{1}{2}m_{\pi^0}^2\phi^2$, which has the form of that of a neutral scalar field, so that it can be used within the relativistic mean-field approach, as it is known that the pion pseudoscalar interaction term vanishes in the mean field level. After some algebra the integration over momenta can be done and the result is

$$Z_b = N^2 \int_{\text{periodic}} [d\phi_1][d\phi_2] \exp\left(\int_0^\beta d\tau \int d^3x \times \left\{-\frac{1}{2}\left[\frac{\partial\phi_1}{\partial\tau} - i(\mu_b - X_0)\phi_2\right]^2 - \frac{1}{2}\left[\frac{\partial\phi_2}{\partial\tau} + i(\mu_b - X_0)\phi_1\right]^2 - \frac{1}{2}(\vec{\nabla}\phi_1)^2 - \frac{1}{2}(\vec{\nabla}\phi_2)^2 + (\partial_i\phi_1)X_i\phi_2 - (\partial_i\phi_2)X_i\phi_1 - \frac{1}{2}(X_i\phi_1)^2 - \frac{1}{2}(X_i\phi_2)^2 - \frac{1}{2}m_b^{*2}\left(\phi_1^2+\phi_2^2\right)\right\}\right), \quad \text{(A8)}$$

where N is a normalization factor. In the mean field approach $\langle X_i\rangle = 0$. Integrating Eq. (A8) by parts, and taking into account the periodicity of ϕ_1 and ϕ_2, the result is

$$Z_b = N^2 \int_{\text{periodic}} [d\phi_1][d\phi_2] \exp\left(\frac{1}{2}\int_0^\beta d\tau \int d^3x \times \left\{\phi_1\left[\frac{\partial^2}{\partial\tau^2} + \nabla^2 - m_b^{*2} + (\mu_b - X_0)^2\right]\phi_1 \times \phi_2\left[\frac{\partial^2}{\partial\tau^2} + \nabla^2 - m_b^{*2} + (\mu_b - X_0)^2\right]\phi_2 + 2i(\mu_b - X_0)\left[\phi_2\left(\frac{\partial\phi_1}{\partial\tau}\right) - \phi_1\left(\frac{\partial\phi_2}{\partial\tau}\right)\right]\right\}\right). \quad \text{(A9)}$$

The fields can be expanded in a Fourier series as

$$\phi_1(\mathbf{x}, \tau) = \sqrt{2}\zeta\cos(\theta) + \left(\frac{\beta}{V}\right)^{1/2}\sum_n\sum_{\mathbf{p}} e^{i(\mathbf{p}\cdot\mathbf{x}+\omega_n\tau)}\phi_{1,n}(\mathbf{p}),$$

$$\phi_2(\mathbf{x}, \tau) = \sqrt{2}\zeta\sin(\theta) + \left(\frac{\beta}{V}\right)^{1/2}\sum_n\sum_{\mathbf{p}} e^{i(\mathbf{p}\cdot\mathbf{x}+\omega_n\tau)}\phi_{2,n}(\mathbf{p}), \quad \text{(A10)}$$

where the Matsubara frequency is $\omega_n = 2\pi nT$, due to the constraint of periodicity of the fields, such that $\phi_k(\mathbf{x}, \beta) = \phi_k(\mathbf{x}, 0)$ for all $\mathbf{x}$. The normalization factors of Eq. (A10) can be chosen so that each Fourier amplitude is dimensionless. The infrared character of the field is carried out by ζ and θ, so that $\phi_{1,0}(\mathbf{p} = 0) = \phi_{2,0}(\mathbf{p} = 0) = 0$, which allows some particles to reside in the $n = 0$, $\mathbf{p} = 0$ state, i.e., a possibility of a condensation of the bosons into the zero-momentum state ("s-wave" condensation). Using Eq. (A10) in Eq. (A9), and noting that $\phi_{-n}(-\mathbf{p}) = \phi_n^*(\mathbf{p})$ because $\phi_1(\mathbf{x}, \tau)$ and $\phi_2(\mathbf{x}, \tau)$ are real fields, we have

$$Z_b = N^2\left[\prod_n\prod_{\mathbf{p}}\int d\phi_{1,n}(\mathbf{p})d\phi_{2,n}(\mathbf{p})\right]e^S, \quad \text{(A11)}$$

where

$$S = \beta V\zeta^2\left[(\mu_b - X_0)^2 - m_b^{*2}\right] - \frac{1}{2}\sum_n\sum_{\mathbf{p}}[\phi_{1,-n}(-\mathbf{p}), \phi_{2,-n}(-\mathbf{p})]\mathbb{D}\begin{bmatrix}\phi_{1,n}(\mathbf{p})\\ \phi_{2,n}(\mathbf{p})\end{bmatrix}, \quad \text{(A12)}$$

and

$$\mathbb{D} = \beta^2\begin{bmatrix}\omega_n^2 + \mathbf{p}^2 + m_b^{*2} - (\mu_b - X_0)^2 & -2(\mu_b - X_0)\omega_n\\ 2(\mu_b - X_0)\omega_n & \omega_n^2 + \mathbf{p}^2 + m_b^{*2} - (\mu_b - X_0)^2\end{bmatrix}. \quad \text{(A13)}$$

As the thermodynamic potential is given by $\Omega = -(1/\beta)\ln(Z)$, we can perform the integrals in Eq. (A11) and write

$$\ln(Z_b) = \beta V\zeta^2\left[(\mu_b - X_0)^2 - m_b^{*2}\right] + \ln\left[(\det\mathbb{D})^{-\frac{1}{2}}\right]. \quad \text{(A14)}$$

The multiplication of Z_b by any constant is irrelevant because it does not change the thermodynamics of the system. The second term of (A14) is given by

$$-\frac{1}{2}\ln[\det\mathbb{D}] = -\frac{1}{2}\ln\left\{\prod_n\prod_{\mathbf{p}}\beta^4\left[\left(\omega_n^2 + \mathbf{p}^2 + m_b^{*2} - (\mu_b - X_0)^2\right)^2 + 4(\mu_b - X_0)^2\omega_n^2\right]\right\} = -\frac{1}{2}\ln\left\{\prod_{n,\mathbf{p}}\beta^2\left[\omega_n^2 + (\omega^+ - \mu_b)^2\right]\right\} - \frac{1}{2}\ln\left\{\prod_{n,\mathbf{p}}\beta^2\left[\omega_n^2 + (\omega^- + \mu_b)^2\right]\right\}, \quad \text{(A15)}$$

so that Eq. (A14) can be written as

$$\ln(Z_b) = \beta V \zeta^2 \left[(\mu_b - X_0)^2 - m_b^{*2}\right] - \frac{1}{2}\sum_{n,\mathbf{p}} \ln\left\{\beta^2\left[\omega_n^2 + (\omega^+ - \mu_b)^2\right]\right\} - \frac{1}{2}\sum_{n,\mathbf{p}} \ln\left\{\beta^2\left[\omega_n^2 + (\omega^- + \mu_b)^2\right]\right\}, \quad \text{(A16)}$$

and in the continuum limit, neglecting the zero-point energy contribution, due to the mean-field approach, the result is

$$\ln(Z_b) = \beta V \zeta^2 \left[(\mu_b - X_0)^2 - m_b^{*2}\right] - V \int \frac{d^3p}{(2\pi)^3} \times \{\ln[1 - e^{-\beta(\omega^+ - \mu)}] + \ln[1 - e^{-\beta(\omega^- + \mu)}]\}, \quad \text{(A17)}$$

where

$$\omega^{\pm}(p) \equiv \sqrt{p^2 + m_b^{*2}} \pm X_0 \quad \text{(A18)}$$

is the effective Bose energy, such that the thermodynamic potential for the bosons is given by

$$\frac{\Omega_b}{V} = -\frac{\ln(Z_b)}{\beta V} = \zeta^2\left[m_b^{*2} - (\mu_b - X_0)^2\right] + T\int \frac{d^3p}{(2\pi)^3}\{\ln[1 - e^{-\beta(\omega^+ - \mu)}] + \ln[1 - e^{-\beta(\omega^- + \mu)}]\}. \quad \text{(A19)}$$

[1] D. J. Gross and F. Wilczek, Phys. Rev. Lett. **30**, 1343 (1973).

[2] J. C. Collins and M. J. Perry, Phys. Rev. Lett. **34**, 1353 (1975); B. Freedman and L. McLerran, Phys. Rev. D **16**, 1130 (1977); **16**, 1147 (1977); **16**, 1169 (1977); V. Baluni, Phys. Lett. B **72**, 381 (1978); Phys. Rev. D **17**, 2092 (1978); S. A. Chin, Phys. Lett. B **78**, 522 (1978); Joseph I. Kapusta, Nucl. Phys. B **148**, 461 (1979); E. V. Shuryak, Phys. Rep. **61**, 71 (1980).

[3] Saeed-uddin, Eur. Phys. J. C **6**, 355 (1999); P. Braun-Munzinger, I. Heppe, and J. Stachel, Phys. Lett. B **465**, 15 (1999); P. Braun-Munzinger, D. Magestro, K. Redlich, and J. Stachel, *ibid.* **518**, 41 (2001); D. Zschiesche, S. Schramm, J. Schaffner-Bielich, H. Stöcker, and W. Greiner, *ibid.* **547**, 7 (2002); F. Becattini, M. Gazdzicki, A. Keränen, J. Manninen, and R. Stock, Phys. Rev. C **69**, 024905 (2004), and many others.

[4] L. McLenan, Rev. Mod. Phys. **58**, 1021 (1986).

[5] B. Mohanty, Nucl. Phys. A **830**, 899c (2009); B. I. Abelev *et al.* (STAR Collaboration), Phys. Rev. C **79**, 034909 (2009), and references therein.

[6] M. Asakawa and K. Yazaki, Nucl. Phys. A **504**, 668 (1989).

[7] A. Barducci *et al.*, Phys. Lett. B **231**, 463 (1989); A. Barducci, R. Casalbuoni, S. DeCurtis, R. Gatto, and G. Pettini, Phys. Rev. D **41**, 1610 (1990); A. Barducci, R. Casalbuoni, G. Pettini, and R. Gatto, *ibid.* **49**, 426 (1994).

[8] M. A. Stephanov, Prog. Theor. Phys. Suppl. **153**, 139 (2004); Int. J. Mod. Phys. A **20**, 4385 (2005); Roberto Casalbuoni, PoSCPOD2006:001, 2006; arXiv:hep-ph/0610179v1.

[9] Z. Fodor and S. D. Katz, J. High Energy Phys. 04 (2004) 050.

[10] R. V. Gavai and S. Gupta, Phys. Rev. D **78**, 114503 (2008); E. Shintani, S. Aoki, and Y. Kuramashi, *ibid.* **78**, 014503 (2008); R. V. Gavai and S. Gupta, *ibid.* **71**, 114014 (2005).

[11] Anyi Li *et al.*, Nucl. Phys. A **830**, 633c (2009).

[12] Philippe de Forcrand, Seyong Kim, and Owe Philipsen, arXiv:0711.0262v3 [hep-lat]; Philippe de Forcrand and Owe Philipsen, JHEP 01 (2007) 077; 11 (2008) 012.

[13] Zoltan Fodor and Sandor D. Katz, JHEP **534**, 87 (2002); 03 (2002) 014.

[14] M. Gaździcki and M. I. Gorenstein, Acta Phys. Pol. B **30**, 2705 (1999), and references therein; M. I. Gorenstein, Phys. Atom. Nucl. **71**, 1594 (2008).

[15] M. Gaździcki, J. Phys. G **30**, S701 (2004); S. Afanasiev *et al.*, Phys. Rev. C **66**, 054902 (2002).

[16] J. Randrup and J. Cleymans, Phys. Rev. C **74**, 047901 (2006).

[17] Y. B. Ivanov, V. N. Russkikh, and V. D. Toneev, Phys. Rev. C **73**, 044904 (2006).

[18] A. S. Khvorostukhin, V. V. Skokov, V. D. Toneev, and K. Redlich, Eur. Phys. J. C **48**, 531 (2006).

[19] A. N. Sissakian, A. S. Sorin, and V. D. Toneev, arXiv:nucl-th/0608032. See also [http://nica.jinr.ru].

[20] S. Chattopadhyay, J. Phys. G **35**, 104027 (2008); P. Senger *et al.*, *ibid.* **36**, 064037 (2009); Johann M. Heuser (CBM Collaboration), Nucl. Phys. A **830**, 563c (2009); see also [http://www.gsi.de/fair].

[21] M. G. Alford, K. Rajagopal, and F. Wilczek, Nucl. Phys. B **537**, 443 (1999).

[22] L. McLerran and R. D. Pisarski, Nucl. Phys. A **796**, 83 (2007); L. McLerran, *ibid.* **830**, 709c (2009).

[23] M. G. Alford, A. Schmitt, K. Rajagopal, and T. Schäfer, Rev. Mod. Phys. **80**, 1455 (2008); R. Casalbuoni and G. Nardulli, *ibid.* **76**, 263 (2004).

[24] L. D. Landau and L. Lifshitz, *Statistical Physics* (Pergamon Press, Oxford, 1969).

[25] H. Müller and B. D. Serot, Phys. Rev. C **52**, 2072 (1995).

[26] H. Müller, Nucl. Phys. A **618**, 349 (1997).

[27] M. Di Toro, T. Gaitanos, V. Greco, and A. Lavagno, Nucl. Phys. A **775**, 102 (2006).

[28] M. Di Toro, B. Liu, V. Greco, V. Baran, M. Colonna, and S. Plumari, Phys. Rev. C **83**, 014911 (2011).

[29] M. Barranco and J. R. Buchler, Phys. Rev. C **22**, 1729 (1980).

[30] N. K. Glendenning, Phys. Rev. D **46**, 1274 (1992).

[31] A. Chodos, R. L. Jaffe, K. Johnson, C. B. Thorne, and V. F. Weisskopf, Phys. Rev. D **9**, 3471 (1974).

[32] N. K. Glendenning, *Compact Stars* (Springer-Verlag, New York, 2000).

[33] B. D. Serot and J. D. Walecka, Adv. Nucl. Phys. **16**, 1 (1986); J. Boguta and A. R. Bodmer, Nucl. Phys. A **292**, 413 (1977).

[34] C. J. Horowitz and J. Piekarewicz, Phys. Rev. Lett. **86**, 5647 (2001).

[35] D. B. Kaplan and A. E. Nelson, Phys. Lett. B **175**, 57 (1986); **179**, 409 (1986); A. E. Nelson and D. B. Kaplan, Nucl. Phys. A **479**, 285c (1988).

[36] P. J. Ellis, R. Knorren, and M. Prakash, Phys. Lett. B **349**, 11 (1995).
[37] R. Knorren, M. Prakash, and P. J. Ellis, Phys. Rev. C **52**, 3470 (1995).
[38] V. Thorsson, M. Prakash, and J. M. Lattimer, Nucl. Phys. A **572**, 693 (1994).
[39] J. Schaffner and I. N. Mishustin, Phys. Rev. C **53**, 1416 (1996).
[40] M. Prakash, I. Bombaci, M. Prakash, P. J. Ellis, J. M. Lattimer, and R. Knorren, Phys. Rep. **280**, 1 (1997).
[41] N. K. Glendenning and J. Schaffner-Bielich, Phys. Rev. C **60**, 025803 (1999).
[42] J. A. Pons, S. Reddy, P. J. Ellis, M. Prakash, and J. M. Lattimer, Phys. Rev. C **62**, 035803 (2000).
[43] Joseph I. Kapusta, *Finite-Temperature Field Theory* (Cambridge University Press, Cambridge, UK, 1989).
[44] J. Cleymans, H. Oeschler, K. Redlich, and S. Wheaton, Phys. Rev. C **73**, 034905 (2006); J. Phys. G **32**, S165 (2006).
[45] P. Danielewicz, R. Lacey, and W. G. Lynch, Science **298**, 1592 (2002).
[46] G. A. Lalazissis, J. König, and P. Ring, Phys. Rev. C **55**, 540 (1997).
[47] K. Sumiyoshi, H. Kuwabara, and H. Toki, Nucl. Phys. A **581**, 725 (1995).
[48] H. Pais, A. Santos, L. Brito, and C. Providência, Phys. Rev. C **82**, 025801 (2010).
[49] B. G. Todd-Rutel and J. Piekarewicz, Phys. Rev. Lett. **95**, 122501 (2005); F. J. Fattoyev and J. Piekarewicz, Phys. Rev. C **82**, 025805 (2010).
[50] N. K. Glendenning and S. A. Moszkowski, Phys. Rev. Lett. **67**, 2414 (1991).
[51] B. Liu, V. Greco, V. Baran, M. Colonna, and M. Di Toro, Phys. Rev. C **65**, 045201 (2002).
[52] F. J. Fattoyev, C. J. Horowitz, J. Piekarewicz, and G. Shen, Phys. Rev. C **82**, 055803 (2010).
[53] T. Klähn *et al.*, Phys. Rev. C **74**, 035802 (2006).